MEMORANDUM
RM-5932-NRL
JANUARY 1969

HUMIDITY AUGMENTATION AS THE INITIAL IMPULSE IN A NUMERICAL CLOUD MODEL

F. W. Murray

PREPARED FOR
OFFICE OF NAVAL RESEARCH

The RAND Corporation
SANTA MONICA • CALIFORNIA

MEMORANDUM
RM-5932-NRL
JANUARY 1969

HUMIDITY AUGMENTATION AS THE INITIAL IMPULSE IN A NUMERICAL CLOUD MODEL

F. W. Murray

This research is supported by the Office of Naval Research under Contract No. N00014-67-C-0101, Reqn. 00178-6-006280. Views or conclusions contained in this study should not be interpreted as representing the official opinion or policy of the Office of Naval Research.

The RAND Corporation
1700 MAIN ST • SANTA MONICA • CALIFORNIA • 90406

PREFACE

The work reported on herein is part of RAND's continuing concern with atmospheric modeling, particularly as it is related to weather modification. The numerical model used for this study was originally developed with rectilinear symmetry, and it used an initial impulse of temperature. In the course of work aimed at improving the model and making it simulate natural clouds more realistically, it was converted to one with axial symmetry, and an initial impulse of relative humidity was tested. The present report is concerned with the implications of the humidity impulse and variations in its size and shape.

RAND's work in cloud modeling has been furthered by the association with the Naval Research Laboratory, which for several years has maintained an active program of observing clouds with the use of instrumented aircraft. Observations made by the Naval Research Laboratory were used in this and previous reports to test the degree to which the model simulates natural clouds.

Previous reports pertinent to this study include RM-5316-NRL, RM-5564-NRL, RM-5582-ESSA, RM-5582/1-ESSA, RM-5870-ESSA and P-3423 (same as Ref. 2).

ABSTRACT

A perturbation of relative humidity is used as a trigger to start the convection process in a numerical model of a cumulus cloud. The effects of varying the width and depth of the perturbation are studied. It is found that the width of the simulated cloud is dependent on the width of the impulse, whereas the ultimate depth and rate of growth are dependent mainly on the depth of the impulse. If a suitable impulse is used, a simulated cloud results that has many of the properties of real clouds observed in an atmosphere with the same basic sounding as the computation.

ACKNOWLEDGEMENTS

Thanks are gratefully extended to J. E. Dinger and R. E. Ruskin of the Naval Research Laboratory for making available results of their field observations of tropical cumuli.

CONTENTS

I. INTRODUCTION

Numerical models of cumulus convection based on direct solution of the equations of hydrodynamics and thermodynamics have a great advantage over models of the entity type in that they do not require specification of a number of arbitrary parameters. Entity models are frequently completely dependent on several such parameters whose values are not well defined either by theory or by experiment; consequently, any desired result can be extracted from them by judicious choice of the parameters. By and large this is not true of the numerical models, but there are some notable exceptions to this statement.

If turbulent diffusion is to be treated explicitly, one or more coefficients must be specified, and theory does not give their values to within one or two orders of magnitude. Certain formulations require explicit turbulent-diffusion terms for computational stability (e.g., Lilly, 1962), but the present model, which is an extension of that of Murray and Hollinden (1966), has sufficient implicit smoothing to be stable with eddy-diffusion coefficients of zero. In the experiments discussed herein, however, a coefficient of 40 m^2 sec^{-1} was used. This is the smallest value found by Ogura (1963) to have any appreciable effect and is also the value favored by Orville (1968) for similar computations.

A much more important arbitrary specification for this type of model is that of the initial impulse. The usual practice is to assume that initially there is no motion and all variables are horizontally uniform. Under these conditions no motion will commence, so some small perturbation must be introduced to initiate convection. In most studies of this type the impulse takes the form of a relatively small region of enhanced temperature, simulating a thermal resulting from solar heating. One disadvantage of this approach in the study of moist convection is that, in the region where the temperature is arbitrarily increased, the relative humidity is correspondingly decreased. Yet, if the convection so initiated is to sustain itself and grow, condensation and release of latent heat must occur, and the lower humidity makes that development all the more difficult. One is

faced with the anomalous situation of trying to grow a simulated cloud in the region of lowest relative humidity (as regards horizontal variation), whereas the physical process generally envisioned for the growth of tropical cumuli is that a series of small convective cells carry moisture aloft into a relatively dry level, each conditioning the air in that limited horizontal region for more vigorous development of the next cell.

A way out of this dilemma is to specify an initial perturbation of relative humidity rather than of temperature. If in a limited region the relative humidity is increased, a horizontal gradient of virtual temperature will result even though the actual temperature remains uniform in the horizontal. But since air density depends on virtual temperature rather than on actual temperature alone, the region with enhanced relative humidity is now more buoyant than its environment. Thus convection can be initiated without the inhibiting effect of arbitrarily depressed humidity. That this mechanism actually operates in nature is confirmed by Vul'fson (1963), who cites measurements by instrumented aircraft over the Black Sea that show ascending air currents to be initiated by horizontal gradients of humidity when the temperature is uniform in the horizontal.

Unfortunately no guidance is available as to the optimum size or strength of a humidity impulse. The arbitrary addition of moisture to the atmosphere is equivalent to the addition of energy to the system, and care must be taken that the energy so added is not so great as to mask the energy conversions that take place during the convection. The present study is meant to give some indication of the effects of humidity perturbations of different sizes and shapes. Limitations of time preclude an exhaustive study of this type, but it is believed that enough information has been obtained to give some useful insights and guidelines for further work in the numerical modeling of tropical cumulus convection.

II. THE MODEL

The equations used and their method of solution have been published in previous reports and will not be repeated here. The basic model is that of Murray and Hollinden (1966). The most important change from that model was the transformation from rectilinear to axial symmetry; the basic mathematical development for this was given by Murray (1967b), and the implications of the change were further investigated by Murray (1968). Briefly, it has been found that all other conditions being identical, the axisymmetric model has faster and more vigorous development than the rectilinear, but its ratio of maximum downdraft to maximum updraft is smaller and more in keeping with observational evidence. Besides the change in the geometry, other minor improvements have been made; the set of equations currently in use is given by Murray (1968).

Once the decision has been made to use a humidity impulse, other decisions must be made as to its exact characteristics. Initially a very simple scheme was used: throughout a horizontal slab extending several hundred meters upward from the presumed cloud base the relative humidity was boosted to 100 percent (or sometimes to 100.4 percent) on the central axis, and to a lesser extent at points successively more distant from the central axis, down to the ambient value at a radial distance of one kilometer, more or less. This worked well enough, but it had a tendency to produce over-vigorous growth.

For the present experiment a somewhat more complicated system was adopted. First, the presumed convective condensation level was determined, and the relative humidity on the central axis was boosted to 100 percent at that level and for 200 to 400 m above it. Next, the relative humidity below the convective condensation level down to the ground was increased so that mixing ratio was constant at its saturation value for the convective condensation level. Next, the relative humidity above the saturated layer was increased so that it varied linearly from 100 percent down to the ambient value at some upper level that was determined by inspection of the basic sounding. The results of these alterations are shown in Fig. 1. The basic

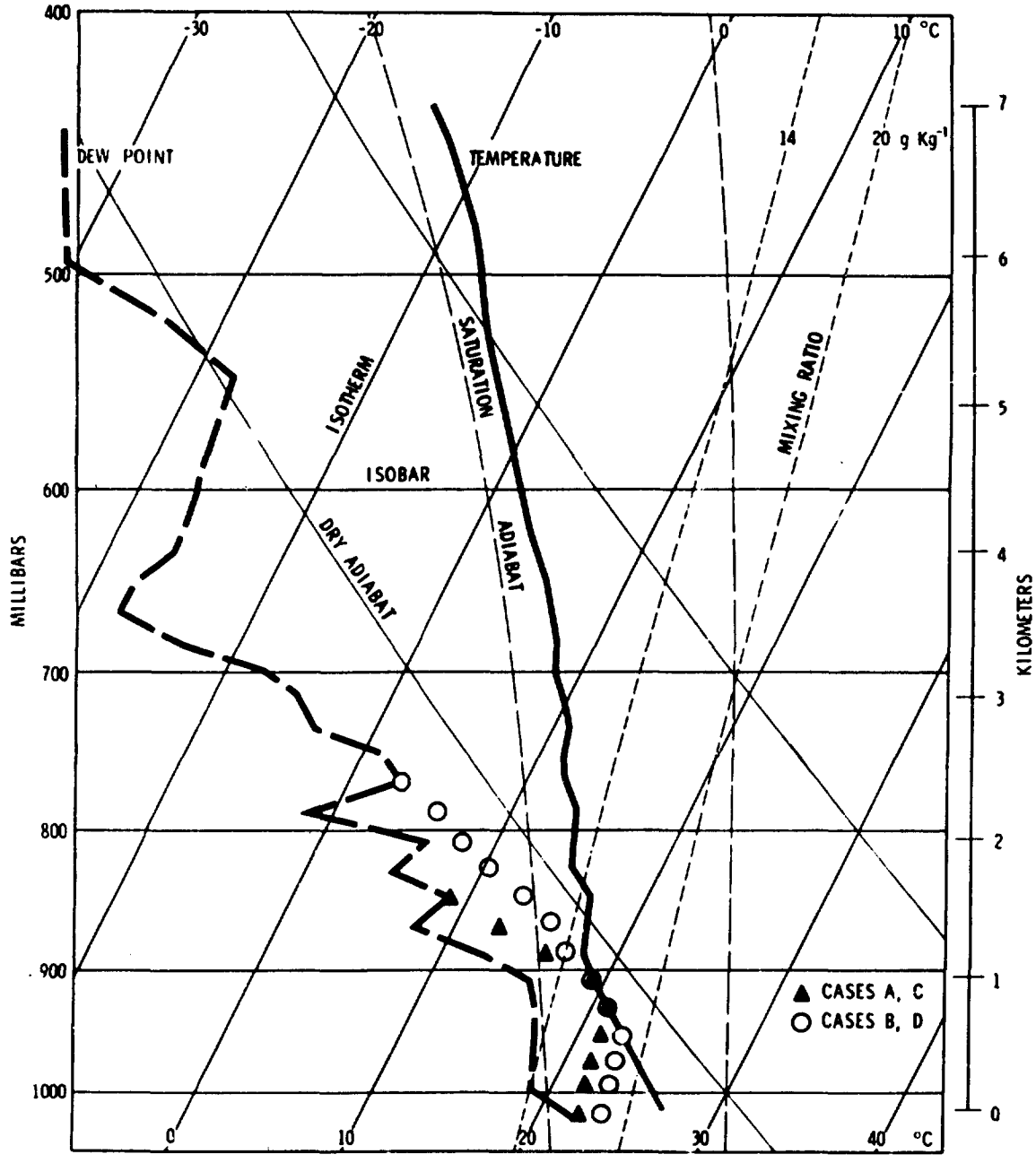

Fig. 1 -- Basic sounding for San Juan, Puerto Rico, 1200Z 17 July 1967. Perturbed humidity values on central axis indicated by triangles and circles.

sounding is for San Juan, Puerto Rico, 1200Z 17 July 1967. Of the four cases considered in the present study, two had the perturbation shown by the triangles, and two had that shown by the circles.

Finally, the perturbation was given width. The boost in relative humidity was slowly diminished linearly with distance from the axis for a few grid intervals, and then diminished to zero according to a cosine dependence. The resulting perturbed relative humidity at a representative level (1 km) for the four cases is shown in Fig. 2.

Two of the cases represent shallow perturbations; and two cases, deep ones. One represents a narrow perturbation; two represent wide ones with a gentle slope; and one represents a wide one with a steep slope. These characteristics are summarized in Table 1.

Table 1.

Case	Depth	Width	Slope	Water Added	
				Total (kg.)	Per unit area (mm of precipitation)
A	Shallow	Narrow	Steep	1,605	2.6×10^{-4}
B	Deep	Wide	Gentle	10,780	3.8×10^{-4}
C	Shallow	Wide	Gentle	6,120	2.2×10^{-4}
D	Deep	Wide	Steep	12,426	8.2×10^{-4}

Also shown in Table 1 is the amount of water added to the system by the perturbation, expressed both as a total amount in kilograms and as the average number of millimeters of rainfall that would occur over the entire area beneath the perturbation if the added water were precipitated out. These figures show that the amount of water added is extremely small in relation to the size of the perturbed region even though in total mass it may appear to be large.

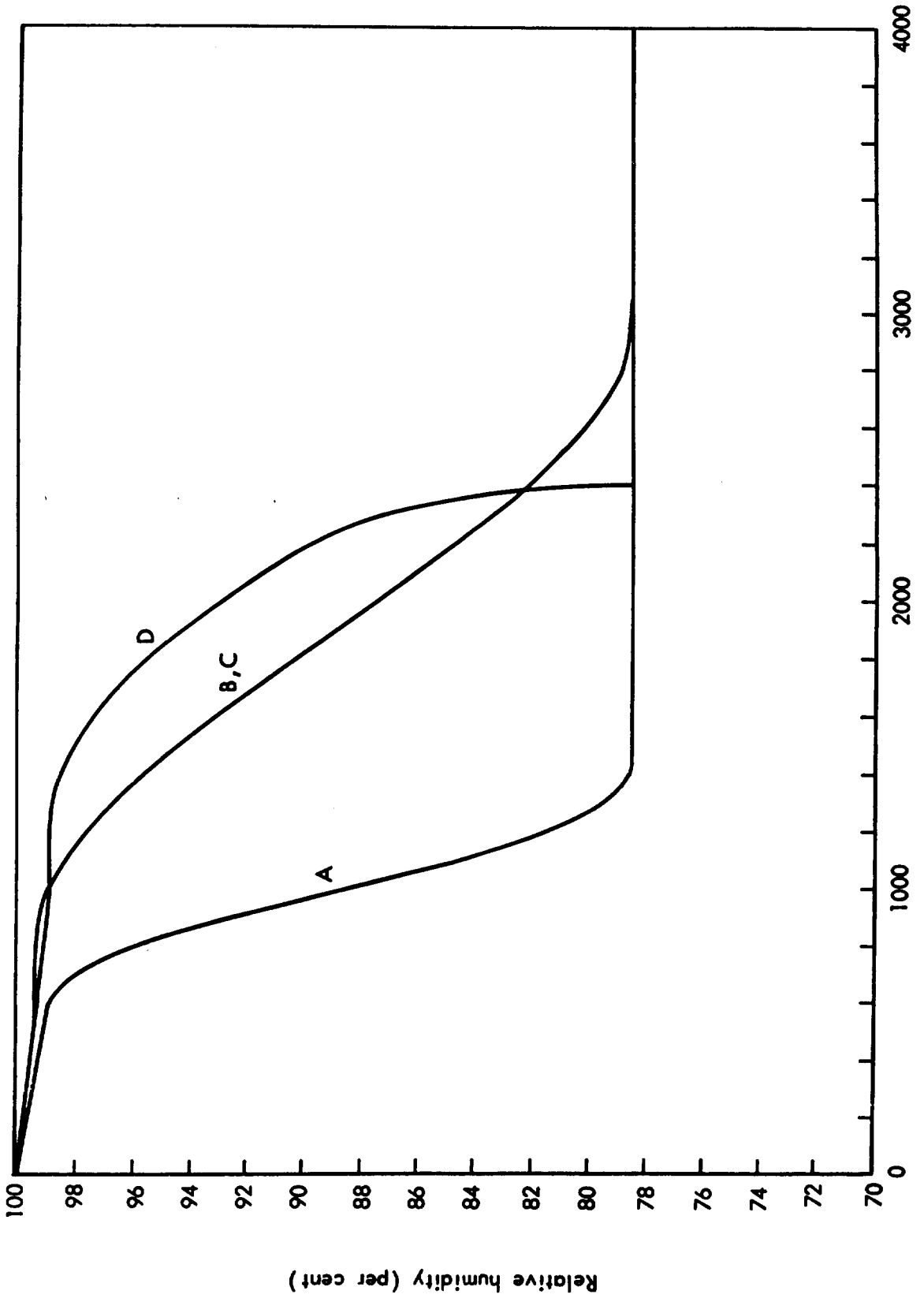

Fig. 2 -- Initial perturbation of humidity at 1 km elevation.

III. DISCUSSION

As a general rule an attempt is made to continue a given run through a number of time steps sufficient to bring the simulated cloud to its decaying stage, or failing this, to carry it until the updraft becomes unreasonably large. Since it is not usually possible to accomplish this in a single session on the computer, the appropriate fields are written out on tape at the end of each time step, making it possible to pick up the computation anew at the point where it was previously interrupted. Unfortunately, tape malfunctions made this impossible for cases C and D, with the result that they ran only 12 and 14 minutes of simulated time respectively. The trend, however, is clear enough from Figs. 5 and 6. Case C, with a shallow perturbation is growing slowly, and will probably reach the decaying stage at a reasonable height and without excessive updrafts. Case D, however, with a deep perturbation, shows almost exponential increase of maximum updraft, with no sign of slacking off.

So far as they go, the short runs C and D resemble the long runs A and B respectively. Fig. 3 shows the maximum updraft in Case A increasing slowly, reaching a peak of nearly 12 m sec^{-1} at 19 minutes and 2600 meters, and dropping sharply thereafter. On the other hand, Fig. 4 shows the maximum updraft in Case B increasing sharply up to the termination of computation, when it is nearly 28 m sec^{-1} at 5800 meters. At any given level the updraft increases very rapidly as the rising cloud vortex passes through that level, and then falls off as rapidly. From Table 1 it can be seen that the perturbation added twice as much water to Case D as to Case C and six times as much to Case B as to Case A, with apparently profound effects on subsequent development.

Comparison of the two shallow perturbations shows that Case A develops faster than Case C, whereas among the two deep ones Case B develops faster than Case D. The difference, however, is not nearly so striking as that between shallow and deep perturbations, and, oddly enough, in both instances the development is faster with the smaller amount of water added. That is to say, for equal perturbation depth

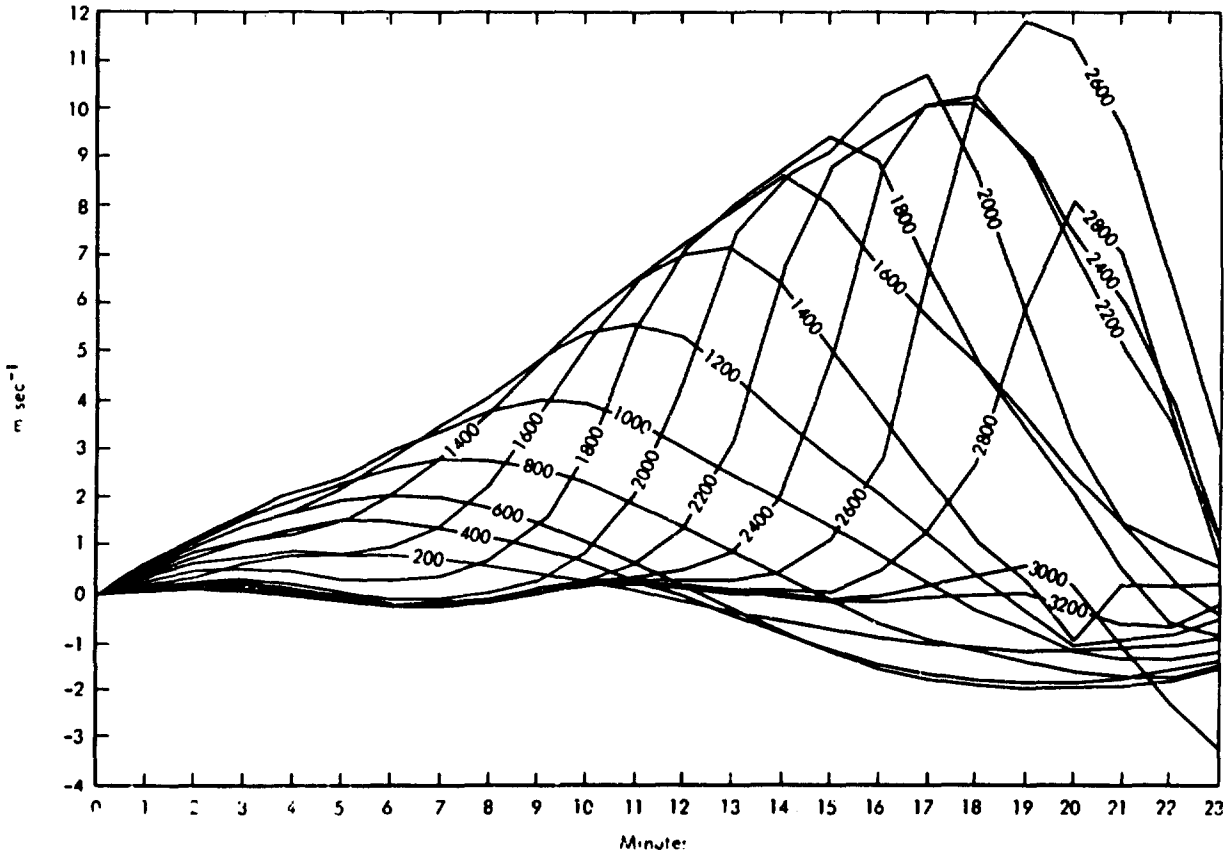

Fig. 3 -- Vertical wind component for several levels on the central axis, Case A.

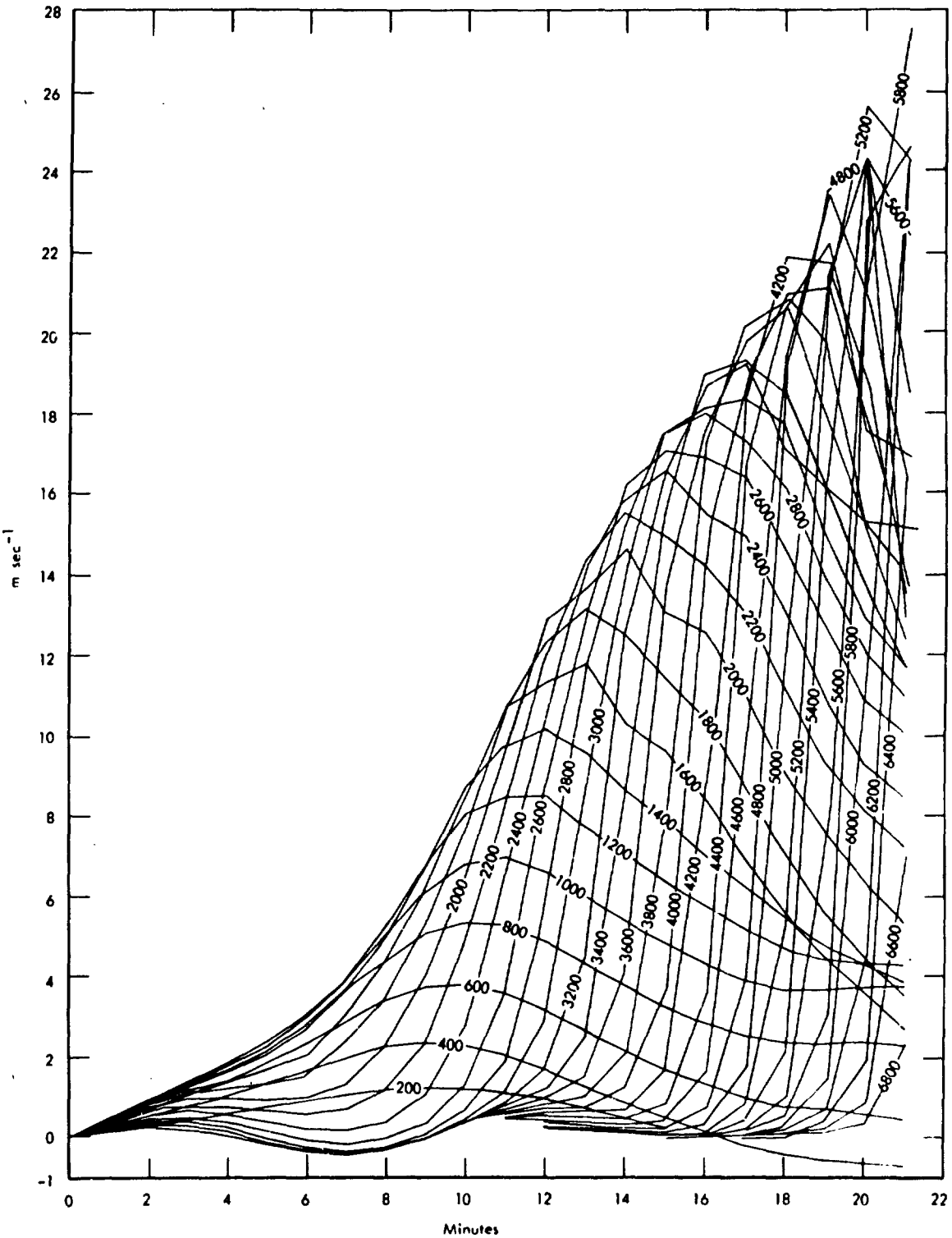

Fig. 4 -- Vertical wind component for several levels on the central axis, Case B.

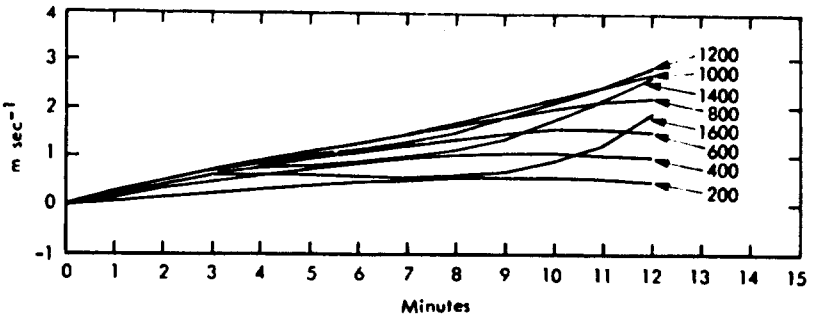

Fig. 5 -- Vertical wind component for several levels on the central axis, Case C.

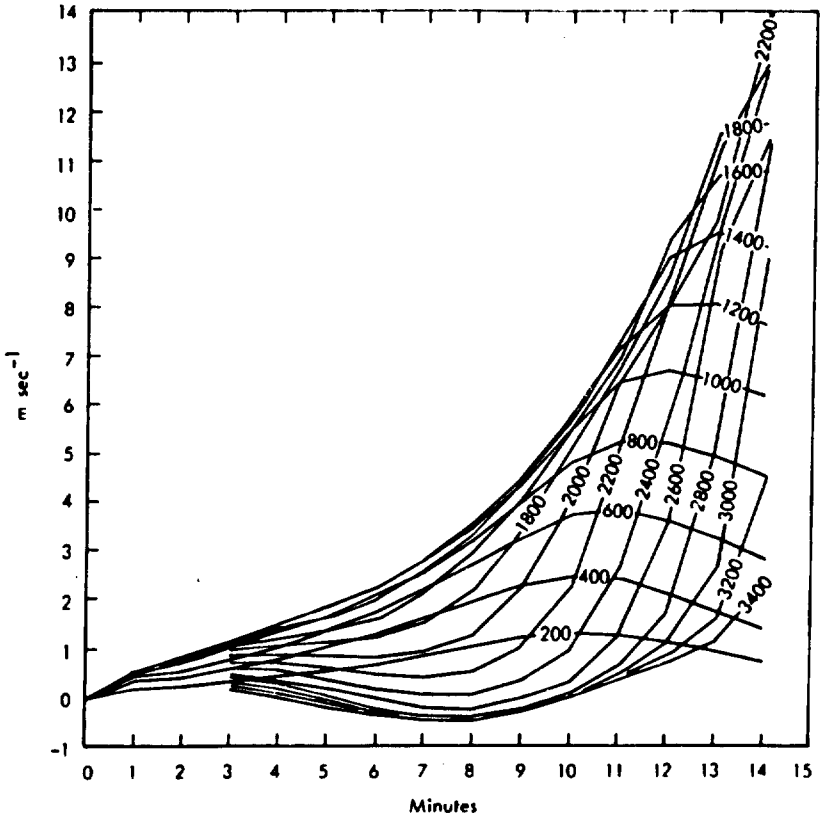

Fig. 6 -- Vertical wind component for several levels on the central axis, Case D.

the development is faster for the narrower perturbation (see Fig. 2). The initial updraft is greatest where the horizontal gradient of virtual temperature is greatest, and narrowing the perturbation brings this zone closer to the central axis. Since the vertical wind is equal to the horizontal derivative of stream function divided by radial distance, it tends to increase as radial distance decreases, other things being equal.

Another way of studying the rate of development is through time sections of mixing ratio of liquid against height along the central axis, Figs. 7-10. It is seen that for Case A (Fig. 7) the cloud top ascends at about 2.2 m sec^{-1}, leveling off near 3 km at 20 minutes. The rate of ascent of the cloud top is fairly uniform from 3 to 17 minutes while the maximum updraft varies from 1.5 to 10.5 m sec^{-1}, averaging 6 m sec^{-1}. A rule of thumb from observation is that the cloud rises at half the speed of the maximum updraft, so the figures in this case seem not to be unreasonable. The cloud base holds steady just below 800 meters during the growing stage, and then starts to rise as dissipation commences. At middle levels within the cloud the slow decrease in the amount of liquid water probably represents turbulent diffusion. The maximum value of 4 g kg^{-1} is quite reasonable.

By contrast, Fig. 8 shows that the cloud top of Case B rose at 2.8 m sec^{-1} during the first 10 minutes and 9.1 m sec^{-1} during the last 10. The water content reached an unrealistic 11.6 g kg^{-1}, there being no precipitation mechanism in the model. The maximum updraft averaged about 4 m sec^{-1} during the first 10 minutes and about 19 m sec^{-1} during the last 10 minutes, still in agreement with the rule of thumb. The magnitudes of the several variables, however, suggest that this case more nearly resembles a thunderstorm than a simple tropical cumulus. This model, at least in its present form, is not well suited for simulating thunderstorms, however.

Figure 9 shows that the amount of condensation and rate of rise of the cloud top are somewhat less for Case C than for Case A. On the other hand, Fig. 10 shows that, as far as it goes, Case D resembles Case B closely in amount and rate of condensation and rise of cloud top.

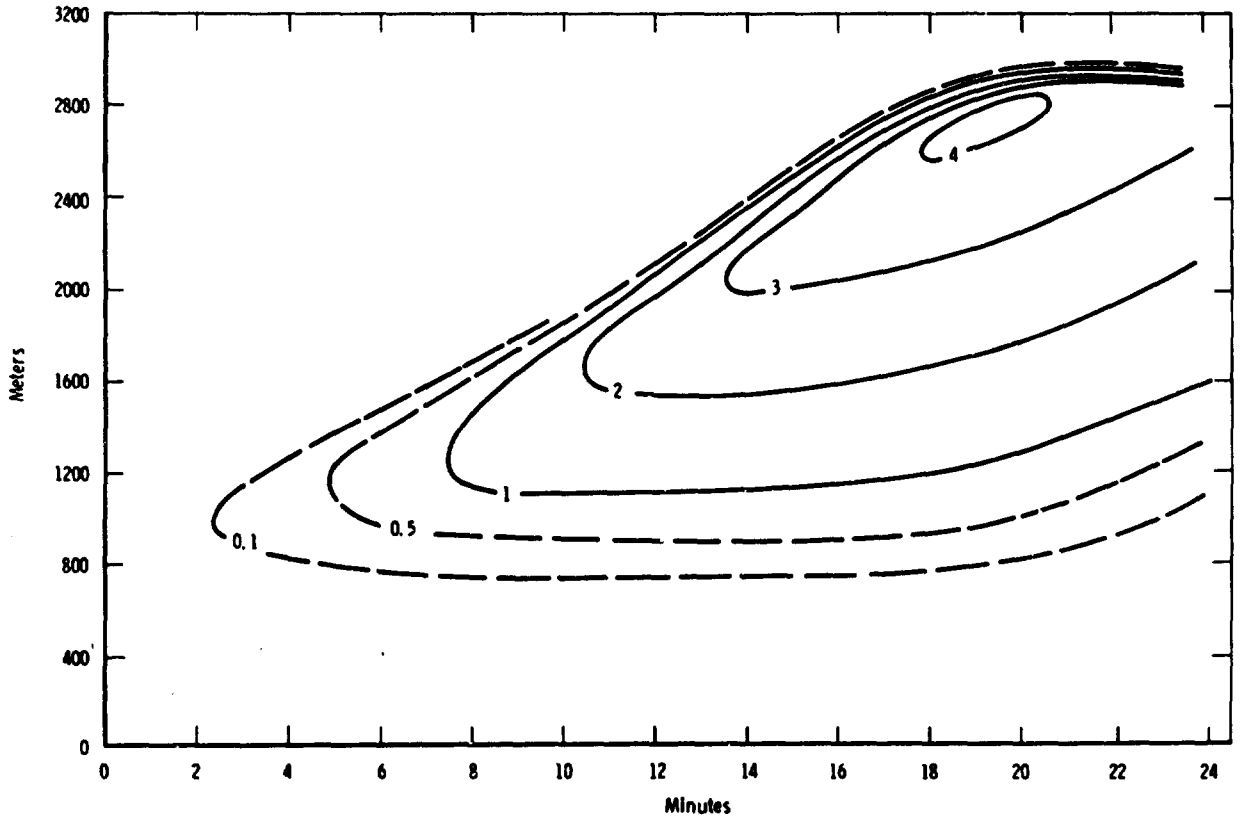

Fig. 7 -- Time section of mixing ratio of liquid, Case A.

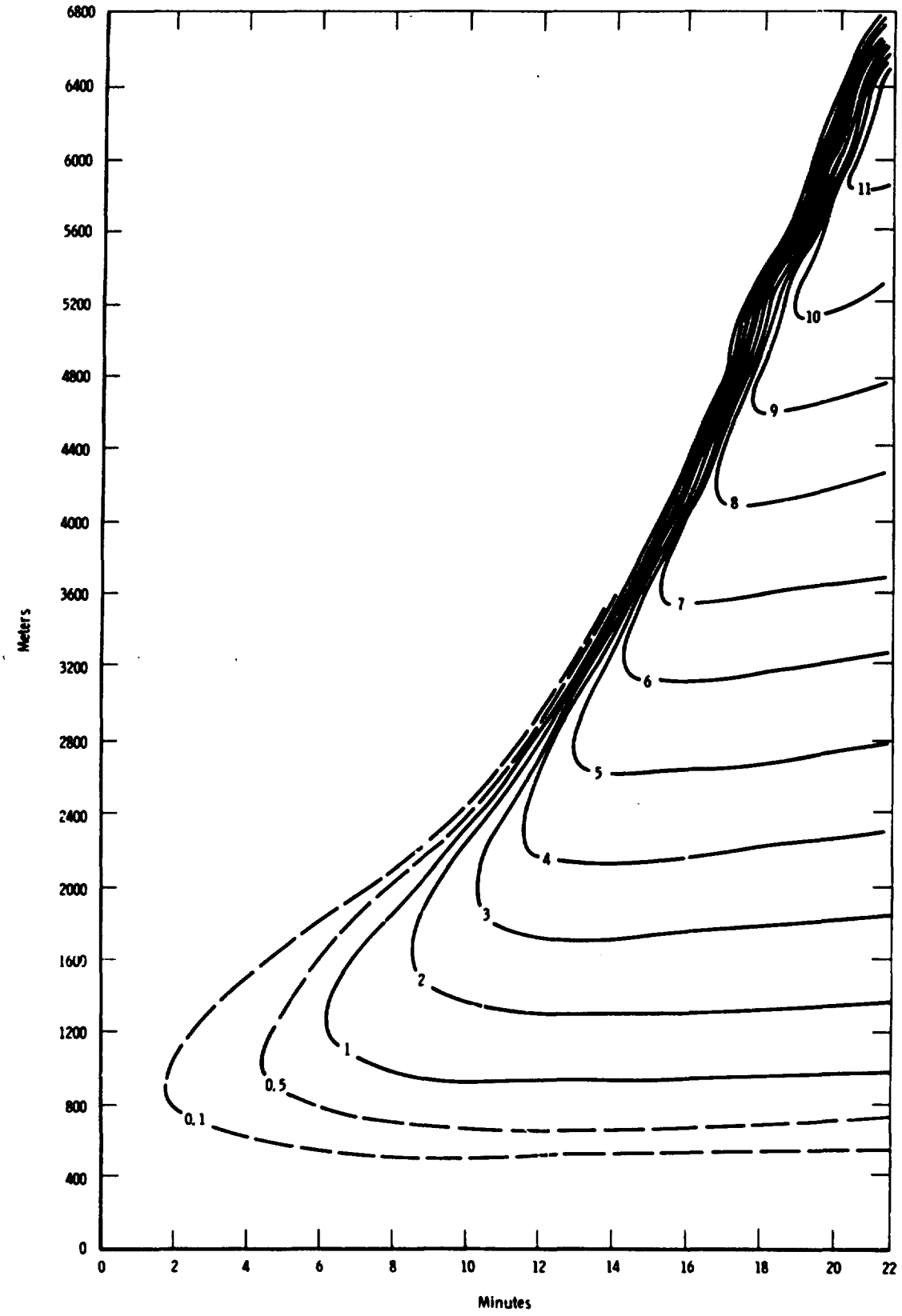

Fig. 8 -- Time section of mixing ratio of liquid, Case B.

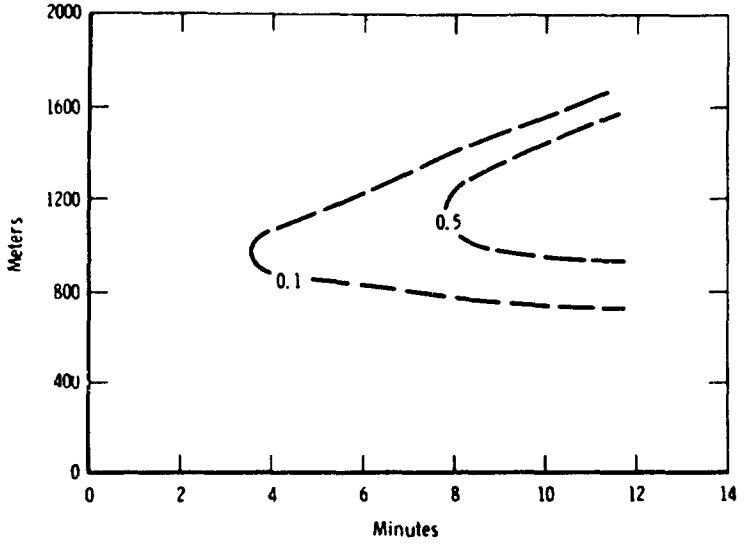

Fig. 9 -- Time section of mixing ratio of liquid, Case C.

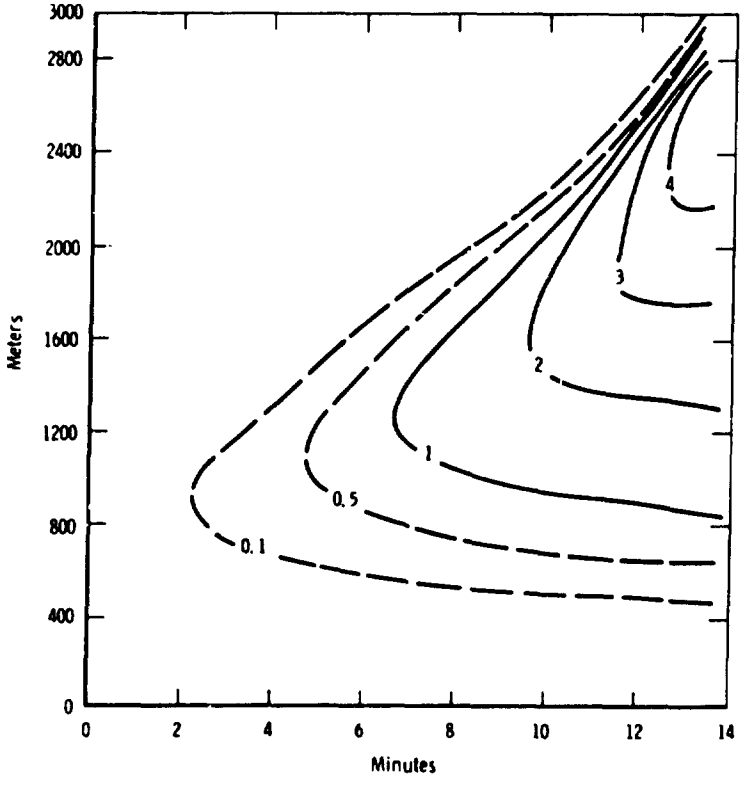

Fig. 10 -- Time section of mixing ratio of liquid, Case D.

It would appear that the radius of the simulated cloud is closely connected with the width of the initial impulse. Comparison of Fig. 11 with Fig. 2 shows that for each of the cases the maximum cloud radius tends to lie between the point where the humidity impulse starts dropping rapidly and the inflection point of the same curve (where the initial horizontal gradient of virtual temperature is at its maximum). This is true regardless of whether the initial impulse is shallow or deep, but it should be noted that the wide, shallow impulse of Case C leads to a wide, shallow cloud.

In both of the runs of long duration the cloud radius starts decreasing even while the cloud is still growing vigorously in depth. This is explainable by the mechanism of evaporation. Murray (1968) noted that though the axisymmetric model has relatively small downdrafts as compared with the updrafts, the downdrafts are concentrated near the outer edge of the simulated cloud, leaving most of the computational region with extremely small vertical motion. The vertical boundary between updraft and downdraft tends to lie within the vertical boundary between liquid and no liquid, that is, within the cloud. Thus, the outermost part of the cloud is subject to evaporation. The eddy-diffusion mechanism also contributes to horizontal shrinkage of the cloud, for it transports liquid outwards to a region more favorable for evaporation. Thus Cloud A, with a radius of 800 meters during its vigorous growth period, has a radius of only 200 meters during its period of decay. More surprisingly, Cloud B reaches a radius of 1600 meters, and then simultanecusly with Cloud A starts shrinking to 800 meters at termination of computation, the period of horizontal shrinkage coinciding with the period of most vigorous vertical growth.

The results indicate that one can safely assert that a wide impulse leads to a wide cloud, but that the ultimate cloud radius depends also on other factors. It is suspected that the total width of the computational region (5800 meters in the present experiments) has a bearing on cloud radius, but this has not been demonstrated.

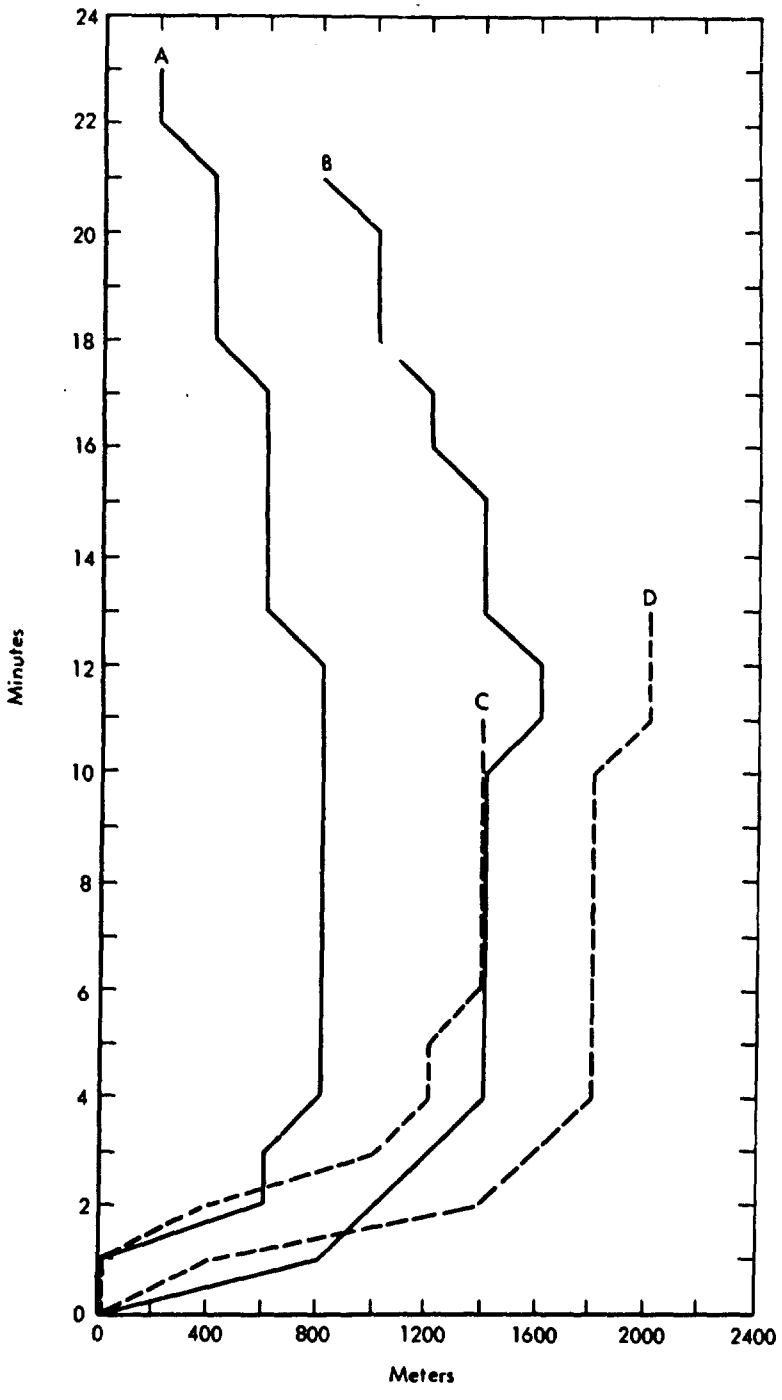

Fig. 11 -- Maximum cloud radius vs. time, four cases.

IV. COMPARISON WITH OBSERVATIONS

The basic sounding (San Juan, Puerto Rico, 1200Z 17 July 1967) was chosen because on that day the Naval Research Laboratory was flying instrumented aircraft in and around clouds in the vicinity. Case A was selected for comparison because of the two long runs it seemed the more realistic. The stronger impulse given to Case B resulted in a cloud that was much deeper than those reported by the Navy observers.

As the variables change in the course of the computation it is possible to read out computed soundings along any vertical at any time. At 19 minutes of simulated time the cloud had reached its peak of development. The computed sounding along the central axis at this time is shown in Fig. 12; it shows the characteristics that one might deduce by applying the parcel method to the initial sounding (Fig. 1). In particular, below the condensation level, the lapse rate has become nearly dry-adiabatic, within the cloud it is very close to the saturation adiabatic, and from the ground surface nearly to the top of the cloud the mixing ratio of total water is constant. (In Figs. 12 and 13 the evaporation dew point is plotted where liquid water exists; see Appendix.) At the top of the cloud the sounding shows the cold cap invariably found in these computations and presumably found in nature as well. This phenomenon results from forced lifting and consequent dry-adiabatic cooling of the air immediately above the top of the cloud. In cases where there is a large temperature excess within the cloud a superadiabatic lapse rate may be found over one or two mesh units, but in the present instance the lapse rate is less steep. This can be attributed to the fact that the initial lapse rate is close to the saturated adiabatic, so little excess temperature can be developed. At higher levels the computed sounding differs little from the observed.

The reason for the close agreement between the computed sounding on the central axis and the results of the parcel method is that the absence of a horizontal component of motion on the central axis precludes dynamic entrainment. Turbulent entrainment occurs through the eddy-diffusion term, but its magnitude is small. Away from the central

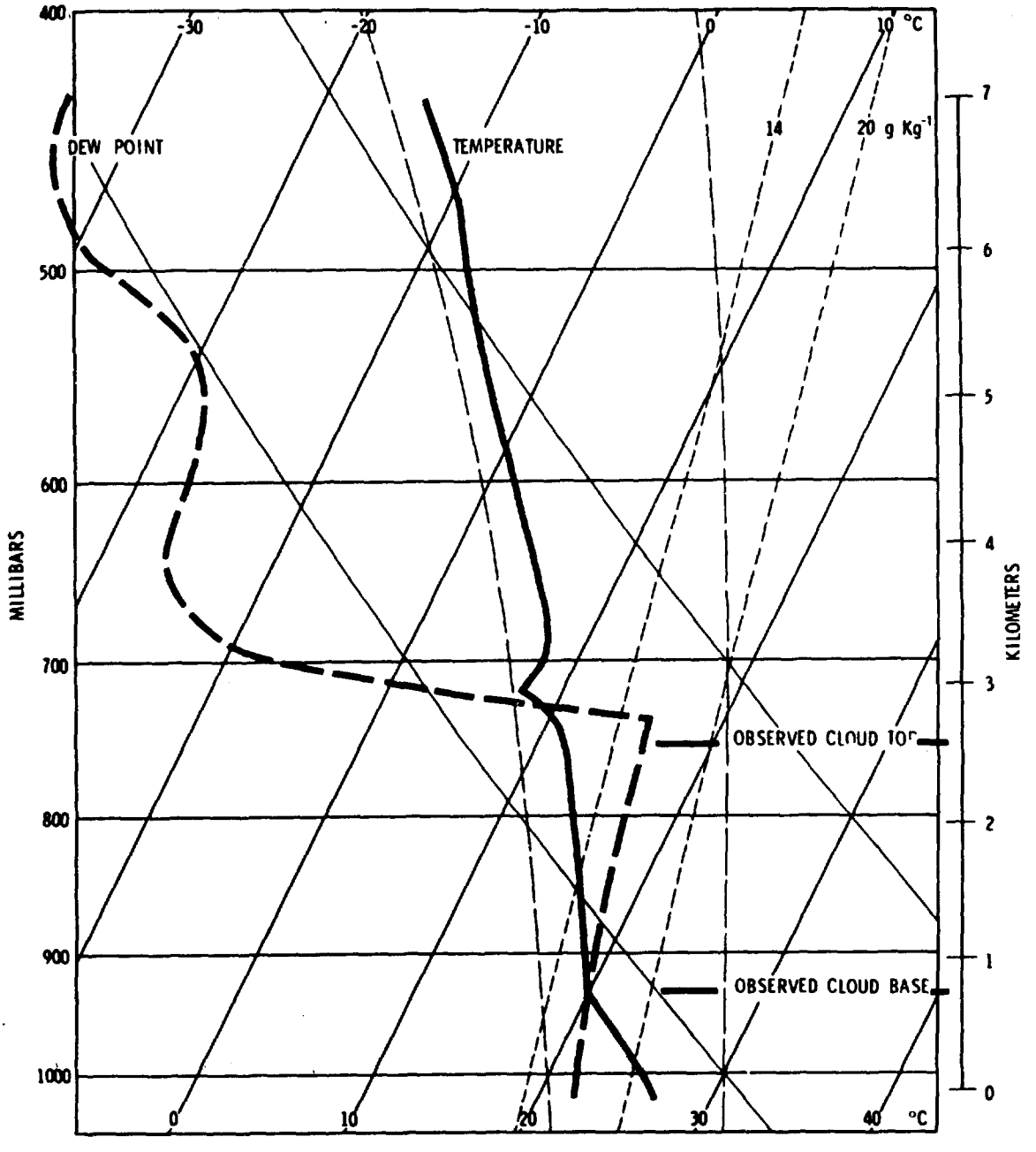

Fig. 12 -- Computed sounding at 19 minutes, on axis, Case A, San Juan, Puerto Rico, 1200Z 17 July 1967.

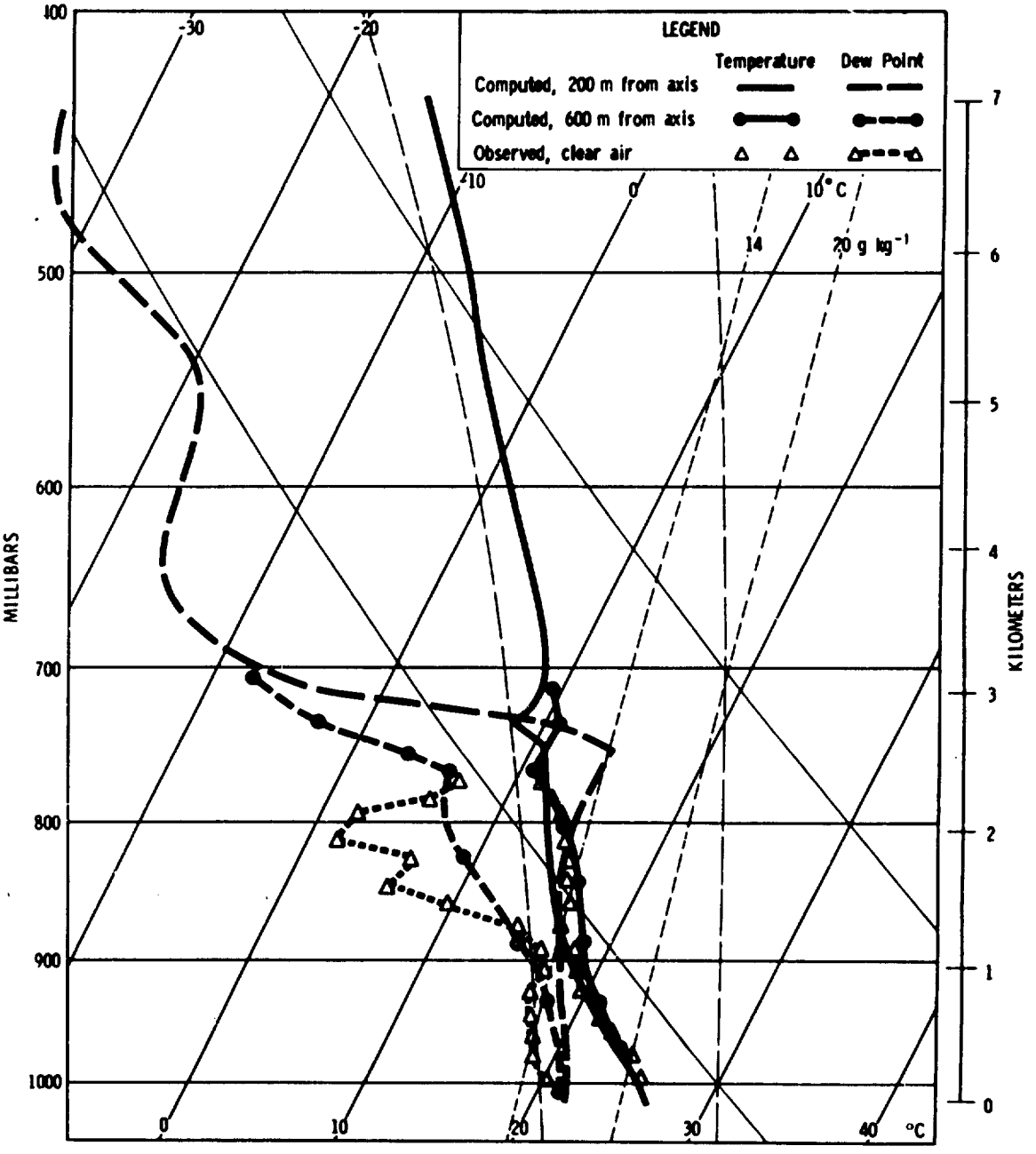

Fig. 13 -- Computed sounding at 19 minutes, off axis, Case A, San Juan, Puerto Rico, 1200Z 17 July 1967. Observations at 1700Z, 40 miles south of Ponce, Puerto Rico.

axis, however, dynamic entrainment can be of major importance. This is illustrated by Fig. 13, which shows the computed soundings 200 and 600 meters from the central axis. The first is within the cloud, but it bears significant differences from that of Fig. 12. The temperature within the cloud is noticeably cooler, and the cold cap is lower and a little less pronounced. The main difference, however, is in the humidity curve, which is well to the dry side of that of Fig. 12, and which shows a decrease with height up to a point near the center of the cloud.

The computed sounding along a vertical outside the cloud, 600 meters from the axis, is quite different. In the lower levels it shows considerable warming, but it, too, shows an effect of the cold cap. The cold air above the cloud is carried outward and downward by the circulation, and it shows distinctly on the clear-air sounding. Incidentally, the upper part of the sounding, just below the cold cap, shows remarkable agreement with an aircraft sounding made during the afternoon 40 miles south of Ponce. The dew-point curve shows fair agreement in its general shape. However, it is less satisfactory than the temperature curve.

Unfortunately, data are not available from aircraft penetrations of clouds on the day of this experiment, but some are for the following day. They indicate that the amount of liquid water present in the simulated cloud is realistic, but a bit high. This is easily explained by the absence of a precipitation mechanism in the simulated cloud. Even if the cloud did not develop to the rain stage, gravitational settling of liquid water would diminish the value in the upper parts of the cloud, perhaps increase it in the lower parts, and cause further cooling below the cloud by evaporation.

Aircraft made several traverses just beneath the cloud base, yielding a limited opportunity for comparison of computation with observation. Temperature and dew-point profiles below a cloud similar in height and width to that of Case A are shown in Fig. 14 together with the corresponding computed profiles. Observed values were not symmetric about the central axis of the cloud; the plotted data are from the half during which the aircraft was moving away from the axis. Even though there was a degree of selection of data for best fit, the

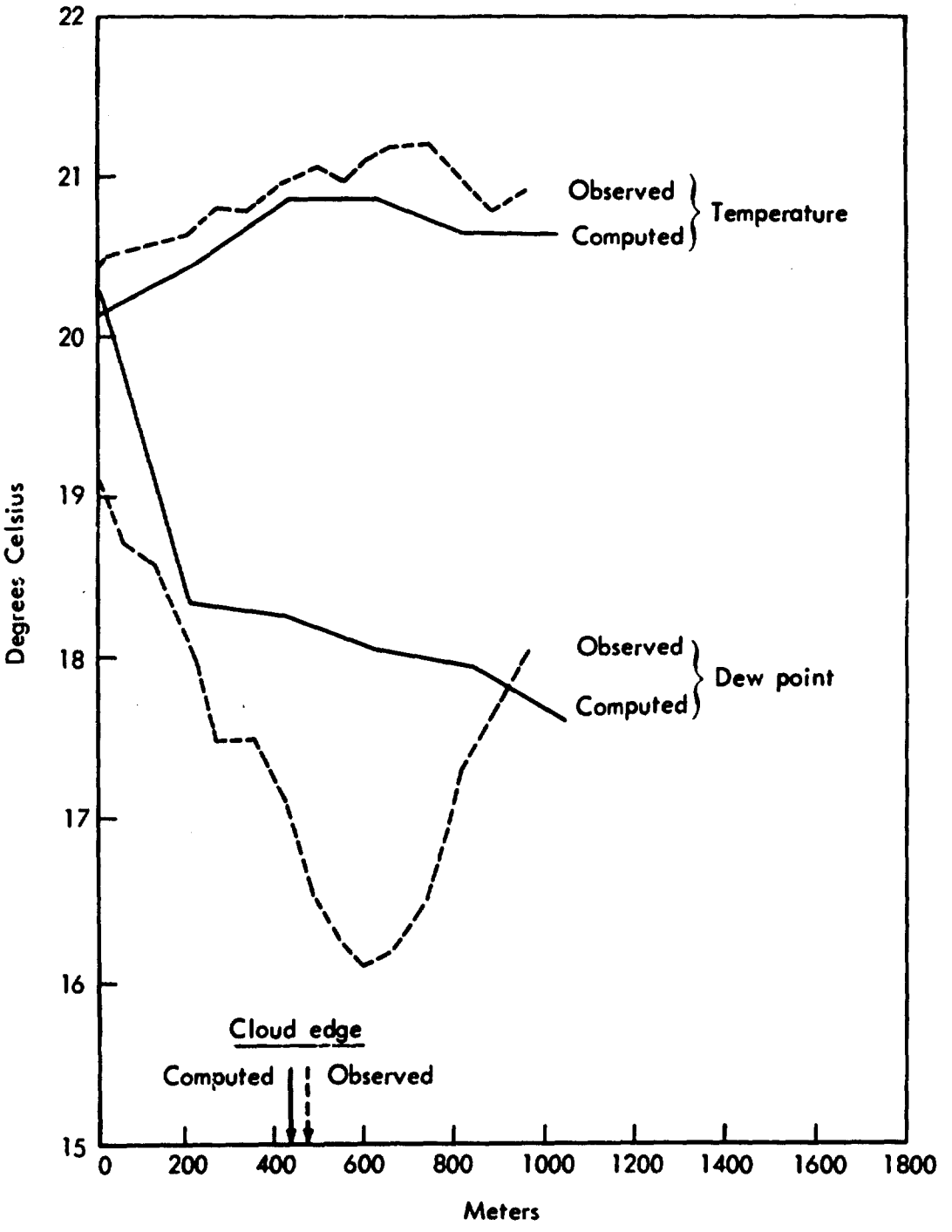

Fig. 14 -- Temperature and dew point immediately below cloud base.

correspondence between computation and observation is not impressive, especially as regards the dew point. The two temperature profiles do remain within a few tenths of a degree of each other and have the same trend -- coldest at the central axis and warmest a few hundred meters beyond the cloud edge. This reflects the warming of the downdraft just outside of the cloud and illustrates a reason for the frequently observed reverse-circulation cell below the cloud. The dew-point curves show a progressive drying with distance from the central axis, but the observed curve reaches a strong mimimum less than 200 meters beyond the cloud edge and then recovers sharply, whereas the computed one continues its decline, but at a moderate rate.

These few items of correspondence between computation and observation are admittedly inadequate, offering little but the assurance that the computational results are not wildly improbable. But the difficulties in getting suitable observational data are formidable indeed. It is very expensive to mount an expedition to measure clouds, and then when the aircraft are deployed it is difficult to find suitable clouds to measure. Moreover, much of the instrumentation is wholly inadequate. There is, for example, no satisfactory way to measure vertical currents in and around clouds, and even for such a quantity as liquid-water content, different types of sensors frequently give widely differing values. Another problem arises from the relatively short life cycle of a cumulus cloud. The computed clouds vary from nothing at initial time through a state of vigorous development to a state of decay in simulated time of about a half-hour, and the same can be said of a natural cloud. But whereas the instantaneous state of development of a simulated cloud can be determined with relative ease, this is not true of a natural cloud. It is frequently difficult to determine just which time step of a cloud simulation to use in making comparisons with observations of a real cloud.

Despite these difficulties it has been possible to make a number of interesting comparisons of observed with simulated clouds. On the whole, these comparisons have led to the belief that the present numerical model is a reasonably good approximation to actual cumulus convection and that further experimentation with it and refinement of it are desirable.

V. CONCLUSION

Earlier work in the numerical simulation of cumulus clouds, both by the author and by others, has almost invariably used local warming as the initial impulse to start the convection. That procedure, however, has certain shortcomings, and so on the basis of theory and some observational evidence the present experiment in the use of a humidity impulse was undertaken.

It was determined that the vigor of the subsequent development of the simulated cloud is closely related to the depth of the humidity impulse. Where the impulse is shallow, the cloud grows slowly, eventually attaining maximum height and maximum updraft speed at reasonable values, and then entering the decaying stage. With the deep impulse, however, the updraft becomes excessively strong with no signs of slacking off, the cloud top rises to an uncomfortable proximity to the upper boundary of the computational region, and the liquid-water content becomes exceedingly high. The deep perturbation adds a great deal more water vapor to the system than does the shallow one, and this water vapor becomes a source of energy for the subsequent development.

This behavior of the model is not unrealistic. The rationale of the humidity impulse is as follows: Over the tropical oceans there is typically a shallow layer of moist air topped by the trade inversion, and surmounted by relatively dry air. Growth of a convective cell beyond the trade inversion is strongly inhibited. However, if a cell does break through, it carries some moisture up into the dry air, introducing a pocket of enhanced humidity. This region, then, is favorable for the development of a later cell, which can transport moisture still higher. Most of the trade cumuli are of strictly limited depth, but if the convective process extends through enough cycles there is an occasional breakthrough leading to a well developed cumulonimbus. Case A of the present experiment can be likened to the ordinary trade cumulus; this is the type of cloud for which Naval Research Laboratory observations are available for this study. On the other hand, Case B represents a cloud in which at the time of initiation moisture had already been carried up through a considerable depth. A vigorous cumulonimbus was the result.

In one-dimensional models, where an entrainment law is assumed such that rate of entrainment decreases with increasing cloud mass (e.g. Simpson, Wiggert, and Mee, 1968), the subsequent height attained by a simulated cloud is directly controlled by the assumed cloud radius; i.e., a wide cloud base leads to a tall cloud. This is a direct outcome of the parcel method modified by progressive dilution of the parcel. The present model, however, does not have such a simple relationship. It is true that the narrow perturbation of Case A led to a narrow cloud of modest height and the wide perturbation of Case B led to a tall, wide cloud. However, the equally wide perturbation of Case C led to a cloud of exceptionally small depth. It is apparent that in this model, cloud depth is much more strongly dependent on impulse depth than on impulse width. The wider impulse does lead to a wider cloud, but its updraft may be smaller than that of a cloud from an impulse of equal width but greater depth. The slope of the impulse has a bearing, too, for the updraft at the first time step is directly dependent on the initial horizontal gradient of virtual temperature.

The weak point of the one-dimensional model of Simpson, Wiggert, and Mee, the strong dependence of results on an initially assumed cloud radius, has its counterpart in the present model in the initial impulse. But since the model is two-dimensional, the initial impulse must also be two-dimensional, and so both a radius and a depth must be assumed together with the two-dimensional distribution of the perturbed quantity within that region. This is not the disadvantage it may seem, however, for it appears that it may be possible to keep the trigger to a size sufficiently small that the subsequent development depends more strongly on the basic sounding than on the impulse. Case B is an example of what ensues when this is not done. Case A is an example of a lesser impulse allowing a simulated cloud to develop with many of the characteristics of the clouds actually observed. Furthermore, the two-dimensional model is free of other arbitrary parameters, such as an entrainment coefficient (the eddy-diffusion coefficient acts as a mild smoother and usually does not affect the results significantly), and it yields considerably more information on the distribution of various properties in and about a cloud than can a one-dimensional model. A three-dimensional model would be better yet, but so far it has been beyond the capacity of available computers.

In general, experience with the humidity impulse has been favorable, but it appears that the later development of the simulated cloud may be more sensitive to the details of this type of impulse than to those of the temperature impulse. It is unfortunate that this is so, for the temperature impulse has some operational drawbacks, and both theory and observation indicate that the humidity impulse may be of great importance in nature. The sensitivity of the model to the impulse need not be a drawback if care is taken to keep the impulse small enough that the major control comes from the basic sounding rather than from the impulse. On the whole, the model with axial symmetry and a humidity impulse seems to give results very close to what is observed in nature, and the way to make further improvements and refinements to the model is clear.

Appendix

EVAPORATION DEW POINT

In plotting soundings through an atmosphere in which liquid water may be present it is advantageous to have a variable that represents the total water, both liquid and vapor. The evaporation dew point is such a variable, and a particularly useful one, for it is easily plotted on a thermodynamic diagram, graphically shows the depth of the cloud, and, moreover, can be directly measured with airborne equipment (Ruskin, 1967).

The numerical model described in this report carries moisture values in the form of mixing ratio. Thus r_v is the mass of water vapor per unit mass of dry air, and r_ℓ is the mass of liquid water per unit mass of dry air. It is desirable to express both ordinary and evaporation dew point in terms of these variables.

The saturation vapor pressure is given by

$$e_s = 6.1078 \exp\left\{\frac{a\,(T - 273.16)}{T - b}\right\} \qquad (1)$$

where T is temperature in degrees Kelvin and

$$a = 17.2693882$$

$$b = 35.86$$

for saturation over water (see Murray, 1967a).

If (1) is solved for T, there results

$$T = \frac{273.16\,a - b\,\ell n\,\frac{e_s}{6.1078}}{a - \ell n\,\frac{e_s}{6.1078}} \qquad (2)$$

The dew point of a parcel of air not containing liquid water is defined as the temperature the parcel would have if cooled isobarically until it is saturated. Thus, if a parcel had vapor pressure e, its dew point T_d would be found by substituting e for e_s and T_d for T in (2), or

$$T_d = \frac{273.16\ a - b\ ln\ \frac{e}{6.1078}}{a - ln\ \frac{e}{6.1078}} \tag{3}$$

The vapor pressure is related to the mixing ratio through

$$r_v = \frac{\varepsilon\ e}{p - e}\ ; \quad e = \frac{p r_v}{r_v + \varepsilon} \tag{4}$$

where p is the total pressure and $\varepsilon = .62197058$ is the ratio of molecular weights of water vapor and air. Combination of (3) and (4) yields

$$T_d = \frac{273.16\ a - b\ ln\left(\frac{p}{6.1078}\ \frac{r_v}{(r_v + \varepsilon)}\right)}{a - ln\left(\frac{p}{6.1078}\ \frac{r_v}{(r_v + \varepsilon)}\right)} \tag{5}$$

If liquid water or ice is present, the evaporation dew point is defined as the ordinary dew point that the parcel would have if all of the liquid and ice were evaporated. Since presumably a parcel containing liquid water or ice is already at the point of saturation, evaporation into it requires an increase of saturation vapor pressure, and consequently through (2) an increase of temperature. Therefore, whereas the ordinary dew point is never greater than the temperature (barring supersaturation), the evaporation dew point is always greater than the temperature unless there is no liquid or ice present, in which case the two dew points are identical.

Let the total mixing ratio be the sum of the mixing ratios of vapor, liquid, and ice, or

$$r = r_v + r_\ell + r_i \tag{6}$$

If all the liquid and ice were evaporated, the value of r would be unchanged, but it would now represent the mixing ratio of vapor; i.e., r_v would increase by the amount that $r_\ell + r_i$ decreased in going to zero. Hence, by comparison with (5) the evaporation dew point is given by

$$T_e = \frac{273.16\ a - b\ \ell n \left\{ \frac{p}{6.1078} \frac{(r_v + r_\ell + r_i)}{(r_v + r_\ell + r_i + \varepsilon)} \right\}}{a - \ell n \frac{p}{6.1078} \left\{ \frac{(r_v + r_\ell + r_i)}{(r_v + r_\ell + r_i + \varepsilon)} \right\}} \qquad (7)$$

Obviously, when $r_\ell + r_i = 0$, (5) and (7) are identical, and $T_d = T_e$.

When soundings were computed for the present report, the dew point was found from (7) with $r_i \equiv 0$. Where the curve of T_e is to the left of the curve of T on the thermodynamic diagrams, $T_d = T_e$. Where the curve of T_e is to the right of the curve of T, it is assumed that $T_d = T$. In this case the difference between the curves of T_e and T read on the mixing-ratio scale of the diagram represents the liquid water.

REFERENCES

1. Lilly, D. K., 1962: "On the numerical simulation of buoyant convection," Tellus, vol. 14, pp. 148-172.

2. Murray, F. W., 1967a: "On the computation of saturation vapor pressure," Journal of Applied Meteorology, vol. 6, pp. 203-204.

3. Murray, F. W., 1967b: Numerical Simulation of Cumulus Convection, Research Memorandum RM-5316-NRL, The RAND Corporation, Santa Monica, California, 34 pp.

4. Murray, F. W., 1968: Numerical Models of a Tropical Cumulus Cloud with Bilateral and Axial Symmetry, Research Memorandum RM-5870-ESSA, The RAND Corporation, Santa Monica, California, 31 pp.

5. Murray, F. W., and A. B. Hollinden, 1966: The Evolution of Cumulus Clouds: A Numerical Simulation and its Comparison Against Observations, Report SM-49732, Douglas Aircraft Company, Inc., Santa Monica, California, 147 pp.

6. Ogura, Yoshimitsu, 1963: "The evolution of a moist convective element in a shallow, conditionally unstable atmosphere: A numerical calculation," Journal of the Atmospheric Sciences, vol. 20, pp. 407-424.

7. Orville, H. D., 1968: "Ambient wind effects on the initiation and development of cumulus clouds over mountains," Journal of the Atmospheric Sciences, vol. 25, pp. 385-403.

8. Ruskin, R. E., 1967: "Measurement of water-ice budget changes at -5C in AGI-seeded tropical cumulus," Journal of Applied Meteorology, vol. 6, pp. 72-81.

9. Simpson, J., V. Wiggert, and T. R. Mee, 1968: "Models of seeding experiments on supercooled and warm cumulus clouds," Proceedings of the First National Conference on Weather Modification, Albany, New York, pp. 251-269.

10. Vul'fson, N. I., 1963: "Effect of air humidity on development of convection in a cloudless atmosphere," English translation in Doklady of the Academy of Science USSR, Earth Sciences Sections, vol. 151 (Published by the American Geological Institute), pp. 10-12.

DOCUMENT CONTROL DATA

1 ORIGINATING ACTIVITY	2a. REPORT SECURITY CLASSIFICATION
THE RAND CORPORATION	UNCLASSIFIED
	2b. GROUP

3. REPORT TITLE

HUMIDITY AUGMENTATION AS THE INITIAL IMPULSE IN A NUMERICAL CLOUD MODEL

4. AUTHOR(S) (Last name, first name, initial)

Murray, F. W.

5. REPORT DATE	6a. TOTAL No. OF PAGES	6b. No. OF REFS.
January 1969	38	10

7. CONTRACT OR GRANT No.	8. ORIGINATOR'S REPORT No.
N00014-67-C-0101	RM-5932-NRL

9a AVAILABILITY / LIMITATION NOTICES	9b. SPONSORING AGENCY
DDC-1	Office of Naval Research (Naval Research Laboratory)

10. ABSTRACT

Discussion of the use of an initial humidity impulse (instead of temperature impulse) in numerical cloud modeling. Experiments use a perturbation of relative humidity to trigger the convection process in an axially symmetrical numerical model of a cumulus cloud. Study of the effects of varying the width and depth of the perturbation shows that the width of the simulated cloud is influenced by the width of the impulse, and its rate of growth and ultimate depth mainly by the depth of the impulse. The initial impulse is an artifice required to start the model. If care is taken not to add large amounts of potential energy in the initial impulse, realistic simulation of cumulus convection can be achieved.

11. KEY WORDS

Meteorology
Weather
Atmosphere
Clouds
Numerical methods and processes
Computer simulation
Models